Stability of scour protection due to earthquake-induced liquefaction

Escribano, Daniella E.; Brennan, Andrew

Published in:
Coastal Engineering

DOI:
10.1016/j.coastaleng.2017.08.015

Publication date:
2017

Document Version
Peer reviewed version

The final version, published in Coastal Engineering is available via DOI: 10.1016/j.coastaleng.2017.08.015

STABILITY OF SCOUR PROTECTION DUE TO EARTHQUAKE-INDUCED LIQUEFACTION: CENTRIFUGE MODELLING

D.E. Escribano[a], A.J. Brennan[b*]

[a]University of Concepción, Department of Civil Engineering, Edmundo Larenas 219, 4030000, Concepción, Chile. Formerly University of Dundee, UK.
[b]University of Dundee, Department of Civil Engineering, Fulton Building, DD1 4HN, Dundee, UK.
*Corresponding author
Email addresses: describano@udec.cl (D.E. Escribano), A.J.Brennan@dundee.ac.uk (A.J. Brennan)

ABSTRACT

A key aspect of permanent offshore structures is protection against scour. This is typically in the form of a blanket of coarse gravel or cobbles surrounding the structure. These coarse particles are selected for their high resistance to being displaced by strong currents and thus protect the underlying finer sand particles from scour. However, in the event of an earthquake, the foundation sand may be susceptible to some degree of liquefaction. This research investigates the effects of seismic-induced liquefaction over a scour blanket, and if sinking is inhibited by some combination of the additional effective stress imposed by the gravel together with the interlocking resistance that develops when coarse particles are subjected to relative displacements.

In order to evaluate the stability of scour protection blankets, a programme of physical modelling was carried out, involving the assessment of different configuration of stone layers over a liquefiable material, and a monopile-type foundation. Models were subjected to scaled base shaking equivalent to earthquake loading. A mass-balance of particle sinkage showed that a filter layer was critical for maintaining the integrity of the armour stones. Based on displacement and pore water pressure measurements, it was found that the presence of the scour protection blankets improved the response of the liquefiable sand under seismic loading, and even inhibited the occurrence of liquefaction. This implied that a well-designed scour protection blanket can assist in protecting against earthquake effects also.

1. INTRODUCTION

One of the major challenges facing offshore structures is the possibility of liquefaction of the seabed. Earthquake loads and strong storms are both major causes of liquefaction in marine deposits. As well, an offshore foundation will be subjected to continuous cyclic loading due to waves during its lifetime, which may progressively lead to liquefaction. Evidence of liquefaction around offshore structures has been reported in the literature. Christian et al. (1974), and Herbich et al. (1984) have reported the phenomenon of floatation of pipelines due to storms produced by liquefaction of the seabed. Miyamoto et al. (1989) reported the subsidence of offshore breakwaters at the Nigata Coast, Japan. Sawicki & Mierczynski (2006) and Sawicki (2014) provide an extensive literature review regarding the practical implications of liquefaction and the dynamics of seabeds and marine structures. Reports on earthquake induced liquefaction in marine structures have been summarized by Sumer et al. (2007). The main differences between wave and earthquake loading is that the stress fluctuation is different (De Groot et al., 2006). In the case of a storm, the loading propagates from the seabed into the subsoil whereas earthquake loading propagates from the ground and moving up to the mud line. Storm waves also have a lower frequency and rather longer durations compared to earthquakes.

A commonly used foundation for marine structures, and especially for offshore wind turbines, is the monopile, which is feasible to install for water depths up to 35 m (Lesny & Hinz, 2007). Because of the effects of currents, and the combined effects of waves and currents, erosion or scouring of the seabed material may occur around such a foundation. The effects of scour produced around an offshore foundation can be mitigated by protecting the soil surrounding the pile with rocks or an armour layer, and its design depends mainly on the shear stresses applied to the soil by currents and waves. To prevent the particles of the seabed soil from washing away through the stones a filter layer can be used, and its design depends on the dimensions of the rock armour and the seabed soil, although this layer is not always considered for scour protections. Figure 1 shows a typical monopile of diameter D_p, surrounded by an armour layer of height t_a and diameter b_a as well as a filter layer between armour and seabed of height t_f and diameter b_f.

Many site investigations indicate that numerous structural failures can be attributed to the effects of wave-induced liquefaction of the seabed, which will affect the scour protection. Physical model tests have been performed to study the pore pressure response around a monopile due to wave action (Sumer et al., 1997; Qi & Gao, 2014), but these were carried out in the absence of the scour protection layer which will affect the response. Previous studies on the effect of liquefaction in the presence of scour protection layers have been focused on the wave-induced liquefaction (Sassa & Sekiguchi, 1999; Sumer et al. 2010) showing that the process of pore pressure build-up and subsequent liquefaction can affect the stability of stone protections (Sassa & Sekiguchi, 1999; Sumer et al., 2010). The experiments of Sassa & Sekiguchi (1999) and Sumer et al. (2010) showed that cover stones such as the ones used for scour protections can sink when the seabed liquefies. Yet, having a cover of stones above the liquefiable layer increases the liquefaction resistance as the stones increase the effective stress of the seabed soil. There remain questions over (i) the effect of seismic loading on scour protection layers, (ii) the effect of scour protection on the liquefiability of the seabed soil and (iii) how this interplays with the presence of a substantial monopile-type foundation.

The aim of this work was therefore to fill this knowledge gap and to study the influence of earthquake shaking and seismic-induced liquefaction on scour protection on offshore foundations. As part of EU funded MERMAID project on the use of Multi-purpose offshore structures, the University of Dundee undertook an experimental study to analyse the effects of dynamic loading upon scour protections. Five centrifuge model tests were carried out on liquefiable seabed soils with different configurations of scour protection layer and foundation. Based on the measured generation and dissipation of excess pore pressure (EPP), the process and mechanism of settlement of the liquefied soil and the stone layers, and a comparison between wave-induced liquefaction and earthquake-induced liquefaction, the principal target is to evaluate the risk of sinkage of scour protection stones in order to inform future design.

2. CENTRIFUGE MODELLING

Small scale physical modelling of larger geotechnical prototypes here would fail to adequately model the important increase in self-weight stresses provided by the armour layers, as well as any inertial stresses induced by soil structure interaction. Therefore, to model effective stresses correctly, the 3 m radius geotechnical centrifuge at the University of Dundee, UK is used. Earthquake loading was achieved using a servo-hydraulic Actidyn Systems QS67-2 in-flight earthquake simulator as described by Brennan et al. (2014). A length scale factor of 1:50 was adopted, and testing correspondingly carried out at 50 times Earth's gravity. The use of this scaling allowed modelling of a 5 m. diameter monopile foundation with scour protection, and with enough soil depth to capture liquefaction phenomena. A schematic diagram of the five tests carried out is shown in Fig. 2; further details about material properties, model preparation and instrumentation are provided below The models were conducted on an equivalent shear beam container, with internal dimensions of 280 mm x 675 mm x 334 mm.

2.1 Material Properties

The sand used to model the seabed was HST95 Congleton sand, which is a specific fraction of the sand extracted at Bent farm, Congleton, Cheshire. It is classified as an even graded fine grained sand and its mineralogical composition consists at 94% quartz (Lauder, 2010). The roundness index (R) is 0.53 (Lauder, 2010) classifying this material as round particle shape. The physical properties of HST95 sand are given in Table 1.

The stones used for scour protection had an irregular shape and two different sizes: D_{50} = 10 mm, and D_{50} = 2 mm, for the armour and filter layers, respectively. The grading, thickness, and extension of each scour protection layer will depend on the design values of waves and currents (Boon et al., 2004). From a scale modelling viewpoint, it was decided that the important factors in the behaviour of this material were that the applied self-weight stresses were appropriate and the ratio of particle size between armour, filter and seabed soils was appropriate. In terms of the design requirements, it is necessary to consider the ratio of average grading (D_{50}) between the seabed D_s and the top layer (D_f: grading size for filter layer; D_a: grading size for armour layer) in order to prevent migration of the seabed material. In this case D_f/D_s =15 and D_a/D_f = 5, which is in the range for the design of scour protections for a monopile foundation of a 6MW offshore wind turbine (Hakfschepel, 2003). Hence, the scour protection particles were scaled to match the grading of the prototype model, and at the same time, the seabed was modelled as a continuum.

2.2 Model Preparation and Instrumentation

For the centrifuge model tests, the seabed sand was placed by air pluviation method. First of all, the sand was passed through a mesh from a storage hopper. The density obtained was continually monitored through the pluviation process in order to maintain a constant value. The models were fabricated with two uniform layers of different relative density I_D and thickness (Figure 2). The achieved I_D varied between 35% and 40% and a thickness of 6.50 m for the loose layer, and I_D between 80% - 83% and thickness of 6.0m for the dense layer.

For the saturation the model container has 5 inlets in the base in order to distribute the pore fluid homogeneously at the bottom of the soil model. The saturation process was carried out slowly under controlled head and flow rate to avoid piping of the soil model and provide uniform saturation.

In order to increase the viscosity of the fluid so that dissipation was correctly scaled at a gravitational acceleration of 50-g, a mixture of de-aired water and Hydroxypropyl methylcellulose (HPMC) was used. The final average viscosity obtained was 50 ±2 cSt.

The different model configurations are shown in Figure 2 at prototype scale; prototype scales are 50 times larger. In the following, all subscript denoted as "*a*" corresponds to the armour layer, and the subscript "*f*" corresponds to the filter layer. The instrumentation consisted of 10 pore pressure transducers (PPTs) and 8 accelerometers (ACCs) to measure excess pore water pressures and horizontal accelerations, respectively. As well, each model had minimum 3 linear variable differential transformers (LVDTs) installed at the surface of the sand, the armour layer, and the filter armour in order to measure their vertical displacement. Square aluminium discs were placed between the surface of the material and the tip of the LVDT to prevent the transducer penetrating into the soil. The square disc sitting in the sand was made with an aluminium mesh in order to allow sand to pass through in case of build-up of pore pressure during testing. With the presence of the stones at the top of the sand, the square disc had an upward-projecting arm as a "telltale", to allow the tip of the LVDT to sit above the soil but still measure the position of the base of the stone layer. The layout of the transducers for all tests is similar, and it is shown for model test S04 in Figure 3.

The stability of scour protection blankets over a liquefiable layer was evaluated first of all, through the analysis of only the sand layers under the two motions imposed (test S01, Figure 2a), followed by a 1D case of an armour scour blanket covering the full extent of the sand surface (test S02, Figure 2b). The influence of a filter layer in a 1D case is considered in test S03 (Figure 2c). A 3D circular sloping profile of protection blanket was modelled in test S04 (M03, Figure 2d), considering both the armour layer and filter layer. Finally, the prototype model presented in Figure 1 is evaluated through test S05 (Figure 2e). Test S05 includes a monopile structure, modelled by a 100mm diameter PVC tube.

Two seismic motions were applied to each model, and the actuator was trained in advance to reproduce these motions with good repeatability (Brennan et al., 2014). The calibrated motions used in this work (Figure 4) consisted of a sinusoidal motion at 2 Hz with an amplitude of 0.1g at prototype model scale, followed by a long wait for pore pressures to reconsolidate, and then a second motion was applied, this one being taken from the 1999 Kocaeli Earthquake (M_s = 7.4) (Izmit Station NGA1165), with a peak input acceleration at prototype scale amplitude of 0.33-g.

3. SEISMIC-INDUCED LIQUEFACTION

3.1 Liquefaction Induced Settlement

Results from tests S01, S02, and S03 (Figures 2a, b and c) are described in this section in order to assess the settlement characteristics of stones with and without a filter layer in a 1 dimensional sense.
Figure 5 shows the excess pore water pressures (EPP) measured with the PPTs at 1.25 m. depth normalized by initial vertical effective stress, r_u, because liquefaction is commonly defined as being commensurate with an r_u value of 1. Figure 5 gives the values of r_u against time for model tests S01, S02, and S03, and motions 1 and 2. The increase in EPP is observed in all test results, with test S01 (no stones) reaching a value of r_u = 1 for motion 1, which indicates full liquefaction. The maximum value of r_u is reduced as the sand is covered by a layer of armour stones (test S02), and slightly less when a filter layer is used (test S03). Peak values of r_u with depth are shown in Figure 6, showing a reduction of r_u at greater depth due to the increase in confining pressure, and below 6.5 m. with an increase in relative density D_r. In all cases it can be seen that r_u decreases as the confining pressure increases. For motion 2 (Figure 6b), the curves for tests S01 and S02 are very similar after the initial depth where the soil liquefied, and for test S03 the values of r_u continue to be lower along the depth of the loose layer. Thus, both the sinusoidal motion and the seismograph produce the same response.

The time of sustained maximum EPP reduces significantly (by a factor of four) for models tests S02 and S03 compared to a liquefiable layer without the presence of a cover of coarse material (Figure 5). The longer periods of elevated EPP may be disadvantageous in terms of damage under earthquake-induced liquefaction, and therefore the use of a cover of stones is beneficial as it decreases the magnitude of maximum EPP generated as well as decreasing the time taken for dissipation to commence. This is interesting because the hydraulic gradients (slope of Figure 6) are similar in all cases, which would suggest that dissipation rates should be similar. However, this would assume that the loose sand in all cases had the same permeability, whereas experimental data on both permeability (Haigh et al. 2012) and consolidation (Brennan and Madabhushi 2011) has shown that soil experiences significant changes in these parameters when r_u approaches unity, and thus by keeping pore pressure ratio below this value then the stones have accelerated the onset of dissipation too.
The gradient of the curves of EPP over time (Figure 5) gives an indication of the rate at which the EPP dissipates. During the phase of EPP dissipation it is observed that the liquefiable layers covered by a coarser layer (tests S02 and S03) have a lower rate of dissipation over time compared to test S01. This observation can be explained by the dissipation front that is progressing from the bottom upwards that has to find its way through the grains of the coarser layers and therefore takes longer to reach the surface. In other words, the stones have finite permeability which has a slight retarding effect on dissipation, but this is a rather secondary effect compared to the reduced time to the start of dissipation noted above.

It is relevant to notice that the previous effects produced by the presence of a coarse layer extend beyond the liquefiable layers depth, and seem to influence the magnitude of EPP produced in the dense layer over 10 m below the surface (Figure 6).

According to the results of EPP, it would be expected that the settlement of the sand will be less for the test using an armour layer, and lesser for the test with the addition of a filter layer. Measured settlements against time are shown in Figure 7. The weight of the cover of stones applies an overburden pressure to the sand which increases the effective stresses and therefore reduces the vertical displacement of the sand during re-consolidation. From the test results shown in Figure 7 it is found that the settlement of the liquefiable layer is reduced by 82% with the presence of the armour layer (1D case), and 86% by using a filter layer.
The shape produced by the settlement of the scour protection after the two motions is shown with dotted lines in Figure 1 and was produced all around the monopile. This deformation pattern is similar than that reported by studies on wave and current induced settlement of scour protections (Lauchlan & Melville, 2001; Nielsen, 2011; Sumer & Nielsen, 2013; Sumer, 2014).

3.2 Stability of Scour Protection

Having assessed the overall behaviour of soil with armour layers, it is important next to evaluate whether failure of the scour material can occur at the particle level. In other words, do the stones sink into the underlying sand? After the tests were performed, the stones were located and their dry weight was calculated, in terms of the amount that sank and the material that remained at the surface of the sand. The graph given in Figure 8 expresses the proportion of stones discovered to have penetrated the sand for all tests with scour protection layers (S02-05, Figure 2). For test with no filter layer S02, 35% of the armour layer material sank into the sand. When using a filter layer below there was no sinking of the armour layer, with 42% and 32 % of the filter layer sinking in models S03 for the 1D case, and S04 for the 2D case, respectively. The total suppression of sinking of the armour layer with the presence of a filter layer proves that its use is highly beneficial for the prevention of sinking due to earthquake-induced liquefaction.

The presence of the monopile in test S05 increased the sinkage, to 4% sinking of the armour layer, and 67% sinking of the filter layer. This is a clear increase from the soil-only tests, and indicative of soil-structure interaction playing a role. Similar to wave-induced liquefaction, the shear stresses moving upwards through the soil due to seismic loading will produce a rearrangement of particles and consequently a densification of the soil layers. The scour protection will be affected by the movement of the bed sediment, which in the worst case scenario the magnitude of settlement will be the combined effect of waves, currents, and a seismic event. Nielsen (2011) analysed the sinking of the scour protections around the monopile foundations of the Horns Rev 1 Wind farm in the North Sea (Hansen et al., 2007, Nielsen, 2007), performing physical experiments of a pile subjected to currents on a wave flume. The scour protections at Horns Rev 1 consist of a 0.5 m thick filter layer with a seabed material of 10 cm mean grain size, followed by a 1.3 m thick layer of stones with a mean grain size of 40 cm. The location of the Horns Rev 1 wind farm presents a seabed of sand with grain size range between 0.1 to 1.0 mm.
The results from a 1D configuration, test S02 and S03, are compared with values of maximum sinking produced by currents from wave flume tests by Nielsen (2011) and in situ monitoring of a monopile at the Horns Rev 1 (Figure 9). The vertical axis indicates the maximum equilibrium sinking experienced by the armour layer h_{max}, which occurs at the sides of the pile and divided by the armour stone size D_a. The horizontal axis indicates the ratio between the thickness of the filter layer t_f and the diameter of the pile D_p, where the value of $t_f/D_p = 0$ means no filter layer used. The use of non-dimensional parameters shown in Figure 9 allows the comparison of the different measurements in terms of the dimensions and characteristics of the scour protection. The two tests considered in this study (S02 and S03) present the maximum sinking in the middle of the model container for the 1D case, and assuming in this case a pile with D_p = 100 mm. The maximum sinking of the armour layer in test S05 was produced adjacent to the

pile of diameter D_p = 100 mm, result that is also included in Figure 9. It is observed that the maximum sinking of the armour layer for the case of seismic motions is two times higher than for the case of current-induced sinking. Nonetheless, the comparisons agree with the effect of using a filter layer which significantly reduce the amount of sinking. The presence of a boundary, in this case the monopile foundation, increases the magnitude of sinking by a further factor (in this case, three times), even with the use of a filter layer (test S05, Figure 9). It is relevant to note that although a filter layer helps to reduce sinking of the armour protection around the monopile, more than half of the filter layer may sink in case of extreme seismic loading (test S05, Figure 8).
Because waves and currents have a progressive effect over the seabed sediments, the maximum sinking of the scour protection may reach a stable condition with no further sinking (Nielsen, 2011). However, this study has shown (Figure 8) that in the event of larger shear stress loading, such as an earthquake, induced liquefaction would appear likely to contribute considerably greater amount of sinking of the scour protection. Based on this data, whilst the presence of a filter layer helps prevent the important armour layer from sinking, it would be prudent to undertake an inspection of the scour protection layers following significant seismic activity in the vicinity of the wind farm.

4. IMPLICATIONS FOR SEISMIC DESIGN OF MARINE STRUCTURES

Figure 10 compares all centrifuge tests, and the vertical displacement experienced by each layer of material. From Figure 8 it was noted that the presence of a filter layer reduced completely the sinking of the armour layer for cases S03 and S04, therefore the magnitudes reflected in Figure 10 are a direct displacement due to the settlement of the sand and filter layers. It is interesting to note that for a 1D case (tests S02 and S03), the presence of a filter layer reduces the sinking of the armour layer but had no influence in the magnitude of sand settlement. The progression from a 1D case to a more realistically shaped protection blanket (2D case, tests S04 and S05), produces an increase in settlement of the scour protections, although no significant changes in the settlement of the sand right beside the monopile. The sinking obtained in the 2D configuration would depend on the lateral extension and thickness of the scour layers. From the results obtained, an increase in the number of filter layers could decrease the maximum EPP experienced by the liquefiable soil and therefore its settlement.

The design guidelines of scour protections consider parameters of waves and current action, as well as the flow patterns around the foundation. Depending on the scour predictions obtained it becomes necessary or not to design a method to mitigate erosion around the monopile. Previous studies related to the generation of EPP in sand due to wave action has been performed by Sumer et al. (2006) on wave-flume tests, and centrifuge performed by Sassa & Sekiguchi (1999). A comparison of the results obtained from the previous studies is given in Fig.11, in terms of the accumulated average pore water pressures normalized by the maximum pore water pressure attained (y-axis, Figure 11), which is a function of different parameters that govern the accumulation of pore pressures during wave loading (Sumer, 2015). For the test data shown in Figure11 from Sassa & Sekiguchi (1999) and Sumer et al. (2006), the equilibrium or maximum pore pressure p_{max} attained by the soil reached the value of overburden pressure σ'_0 and therefore experienced liquefaction. The angular frequency of the waves normalized by time (x-axis at logarithmic scale for comparison purposes, Figure11) represents the number of cycles at which pore pressures progress during loading. Tests S01 and S02 were included for comparison with the phenomena of wave-induced liquefaction and earthquake-induced liquefaction in terms of pore pressure build-up. Figure 11 shows that 1-g wave flume tests and 50g centrifuge tests give similar results for wave-induced pore water pressure. Although during dynamic loading the liquefied layer reaches p_{max} at a much faster rate, it will also dissipate EPP fast enough to then reconsolidate. The presence of stones reduces the velocity of pore water pressure build-up, but only showing marked differences over an accumulated average pore pressure ratio of 0.7 compared to wave loading. The previous comparison gives a preliminary method to combine the effects of wave loading and seismic loading into the analysis of liquefaction phenomena in marine environments.

5. CONCLUSIONS

The stability of scour protection layers has been analysed with results from dynamic centrifuge model tests. Typical dimensions of scour protection for a 6 MW offshore wind turbine were used at a scale of 1:50. The analysis involved measurements of settlement and excess pore water pressure generation during and after dynamic loading. The following conclusions can be drawn:

(a) The presence of a cover of stones, with and without the presence of a filter layer, accelerates the dissipation of EPP after dynamic loading. This effect is experienced in the liquefiable layers as the application of an overburden pressure above reduces the ratio r_u below unity, and therefore inhibiting liquefaction. This response was observed to extend beyond the depth of the liquefiable layers.

(b) The induced settlement of the liquefiable layers due to seismic loading was reduced by almost three times compared to the case of no scour protection, as a result of a slight increase in effective stresses due to the presence of an armour layer, with an without filter layer.

(c) The stability of the armour protection layer was highly improved by the use of a filter layer, with a reduction of over 96% the settlement of stones, for a mean grain size ratio D_a/D_f of five. Conversely, the filter layer was significantly affected by dynamic loading, with more than 50% settlement with the presence of a monopile structure. Additionally, the effect of seismic loading on the scour protection layers compared to wave and current loading (Figure 9), may increase sinking up to four times. Design guidelines should consider the presence of armour and filter layers in areas prone to seismic action and inspection measures post-earthquake.

(d) The effect of layers of stones above a liquefiable material improve substantially the magnitude of settlement as well as reducing the effect of EPP which, for this configuration, inhibited the phenomena of liquefaction. The presence of a monopile-type foundation has no significant effect on the sinking of the liquefiable sand, although the scour protection, specifically the filter layer, had 67% of its total weight sinking into the liquefiable material.

(e) Future design of monopile foundations in seismic prone areas should consider the beneficial effects of scour protections over the settlement and the prevention of liquefaction effects. The similarities of pore pressure progression with time between wave and seismic action gives a starting point to the introduction of seismic loading parameters into the design of scour protections for offshore foundations.

6. ACKNOWLEDGEMENTS

This work was funded through the EU FP7 programme as part of the project “MERMAID - Innovative Multi-purpose off-shore platforms: planning, design and operation” OCEAN.2011-1 Grant Agreement no: 288710. Technical assistance in the centrifuge tests from the Geotechnical Laboratory at UoD, is greatly appreciated.

7. REFERENCES

Bertalot, D. (2013). *Seismic behaviour of shallow foundations on layered liquefiable soils*. PhD thesis, Dept. of Civil Engineering, University of Dundee, UK.

Brennan, A.J. & **Madabhushi**, S.P.G. (2011). *Measurement of Coefficient of Consolidation during Reconsolidation of Liquefied Sand*. Geotechnical Testing Journal, Vol. 34, No. 2.

Brennan, A.J., Knappett, J.A., Bertalot, D., Loli, M., Anastasopoulos, I. & Brown, M.J. (2014) *Dynamic centrifuge modelling facilities at the University of Dundee and their application to studying seismic case histories* Proceedings of the 8th International Conference on Physical Modelling in Geotechnics, Perth, January 2014. 227-234

Christian, J.T., Taylor, P.K., **Yen**, J.K.C., **Erali**, D.R. (1974). *Large diameter underwater pipeline for nuclear power plant designed against soil liquefaction*. Proceedings of Offshore Technology Conference, Dallas, pp. 597-606.

Groot, **de**, M., **Bolton**, M., **Foray**, P., **Meijers**, P., **Palmer**, A., **Sandven**, R., **Sawicki**, A. & **Teh**, T. (2006). *Physics of liquefaction phenomena around marine structures*. Journal of Waterway, Port, Coastal and Ocean Engineering, 132. Pp. 227-243.

Hansen, E.A., **Simonsen**, H.J., **Nielsen**, A.W., **Pedersen**, J., and **Høgedal**, M. (2007). *Scour protection around offshore wind turbine foundations, full-scale measurements*. In Scientific Proceedings of the European Wind Energy Conference 2007 (EWEC 2007), 132-138. Nielsen, A.W. and Hansen, E.A. (2007).

Herbich, J.B., **Schiller**, R.E. Jr., **Watanabe**, R.K. and **Dunlap**, W.A. (1984). *Seafloor Scour. Design Guidelines for Ocean-Founded Structures*. Marcell Dekker, Inc., New York, NY, xiv + 320p.

Lauder, K. (2010). *The performance of pipeline ploughs*. PhD thesis, Dept. Civil Engineering, University of Dundee, UK.

Lauchlan, C.S. & **Melville**, B.W. (2001). *Riprap protection at bridge piers*. Journal of Hydraulic Engineering, Vol. 127(5), pp. 412-418.

Lesny, K., Hinz, P. (2007). Investigation of monopole behaviour under cyclic lateral loading. 6th International Offshore Site Investigation and Geotechnics Conference, London, England, pp. 383-390.

Miyamoto, T., **Yoshinaga**, S., **Soga**, F., **Shimizu**, K., **Kawamata**, R. and **Sato**, M. (1989). *Seismic prospecting method applied to the detection of offshore breakwater units settling in the seabed*. Coastal Engineering in Japan, vol. 32, No. 1, pp. 103-112.

Nielsen, A.W. and **Hansen**, E.A. (2007). Time-varying wave and current induced scour around offshore wind turbines. In Proceedings of the International Conference on Offshore Mechanics and Arctic Engineering – OMAE, Vol. 5, pp. 399-408.

Nielsen, A.W. (2011). Scour protection of offshore wind farms. PhD thesis, Dept. of Mechanical Engineering, Technical University of Denmark.

Qi, W.G., & **Gao**, F.P. (2014). Physical modelling of local scour development around a large-diameter monopile in combined waves and current. Coast Eng. VVol.83, pp. 73-81.

Sassa, S. & **Sekiguchi**, H. (1999). *Wave-induced liquefaction of beds of sand in a centrifuge*. Geotechnique, Vol. 49, No. 10, pp. 621-638.

Sawicki, A. & **Mierczynski**, j. (2006). *Developments in modelling liquefaction of granular soils caused by cyclic loads*. Applied Mechanics Reviews, Vol. 59, March issue, pp. 91-106.

Sawicki, A. (2014). *Mechanics of seabed liquefaction and resolidification*. Archives of Mechanics.

Stewart, D.P., **Chen**, Y.R. and **Kutter**, B.L. (1998). *Experience with the use of methylcellulose as a viscous pore fluid in centrifuge models*. Geotechnical Testing Journal, 21(4), pp. 365-369.

Sumer, B.M., **Hatipoglu**, F., **Fredsoe**, J. and **Sumer**, S.K. (2006). *The sequence of soil behaviour during wave-induced liquefaction*. Sedimentology, Vol. 53, pp. 611-629.

Sumer, B.M. & **Nielsen**, A.W. (2013). *Sinking failure of scour protection at wind turbine foundation*. Proceedings of the ICE, Vol. 166, Issue EN4. pp. 170-188.

Sumer, B.M. (2014). *Liquefaction around marine structures*. Advanced Series on Ocean Engineering. Vol. 39. World Scientific.

Sumer, B.M., **Christiansen**, N. and **Fredsoe, *J. (***1997). *Horseshoe cortex and vortex shedding around a vertical wall-mounted cylinder exposed to waves*. J. Fluid Mechanics, Vol. 332, pp. 41-70.

Table 1. Physical properties of HST95 Congleton sand.

Property	Bertalot (2013)
D_{10} (mm)	0.07
D_{30} (mm)	0.10
D_{60} (mm)	0.146
C_u	1.96
G_s	2.63
$\gamma_{d,min}$ (kN/m^3)	14.34
$\gamma_{d,max}$ (kN/m^3)	17.60
e_{max}	0.795
e_{min}	0.463

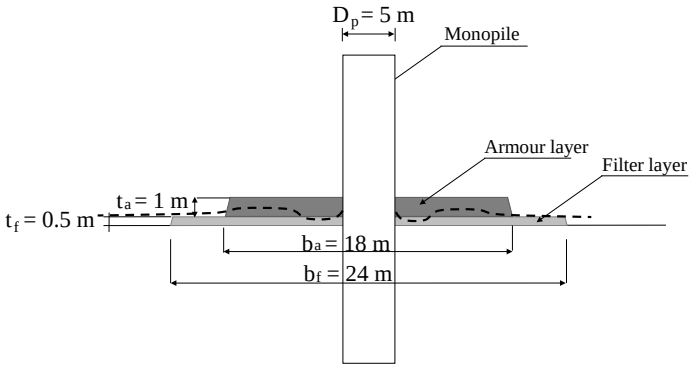

Figure 1. Sketch of monopile foundation with scour protection. Armour layer deformation represented by dotted lines.

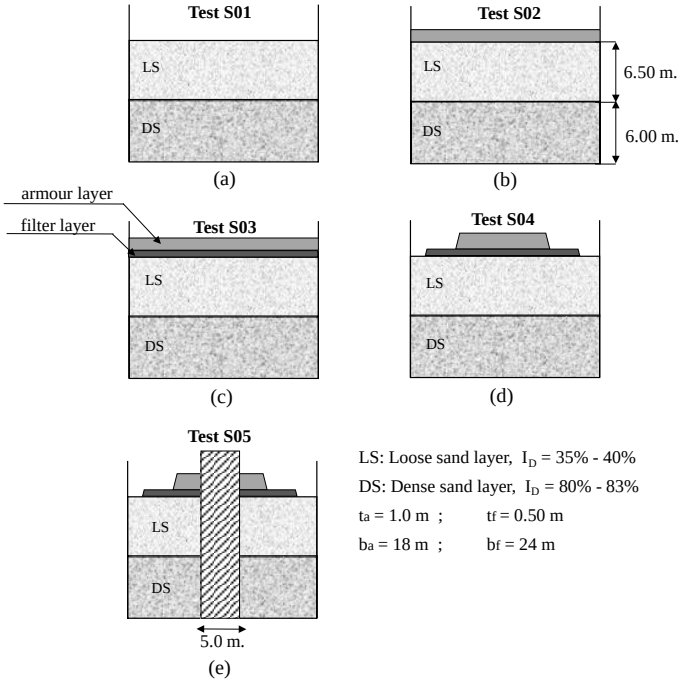

Figure 2. Centrifuge models layout (thickness and diameter of the protection layers shown in prototype scale).

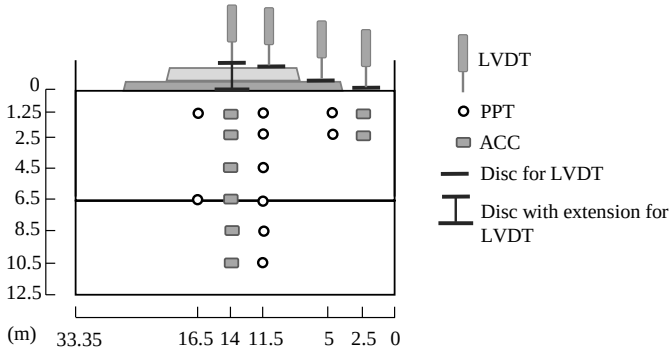

Figure 3. Distribution of transducers for test model S04. Dimensions at Prototype scale.

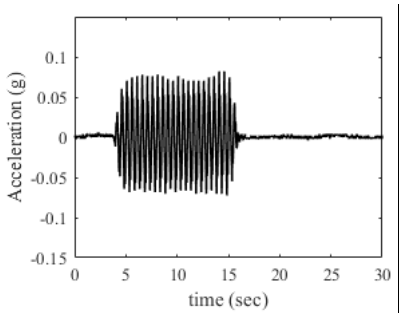

Figure 4(a). Motion 1, time domain.

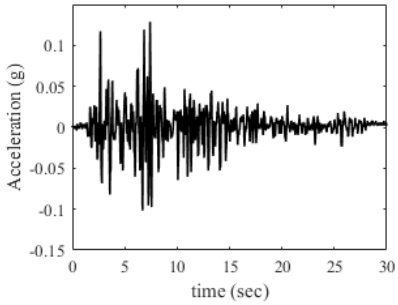

Figure 4(b). Motion 2, time domain.

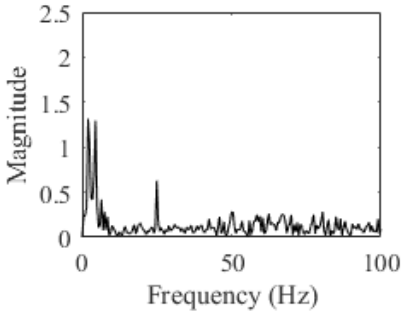

Figure 4(c). Motion 1, frequency domain

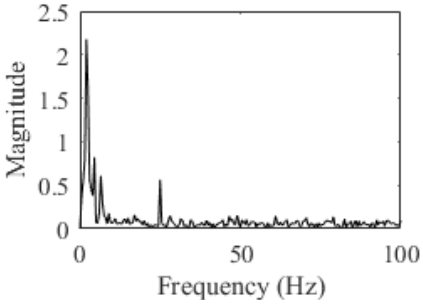

Figure 4(d). Motion 2, frequency domain.

Figure 4. Input motions in the time domain and frequency domain at Prototype scale.

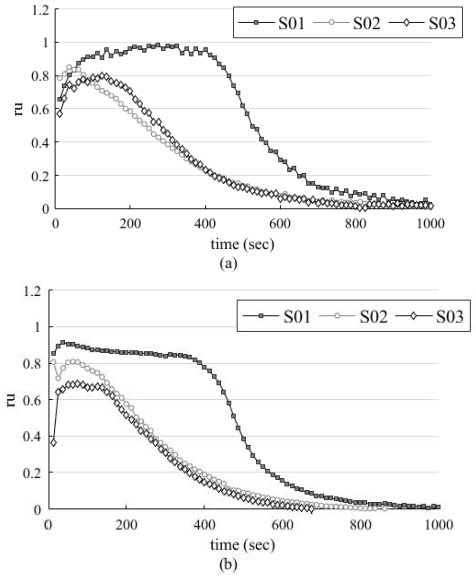

Figure 5. Ratio r_u against time for a prototype depth of 1.25 m: (a) Motion 1 Sinusoidal; (b) Motion 2 Kocaeli Earthquake.

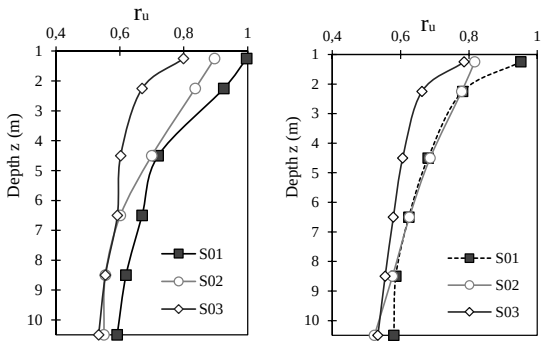

Figure 6 (a) Motion 1 *Figure 6(b) Motion 2*

Figure 6. Excess pore pressure ratio r_u against time.

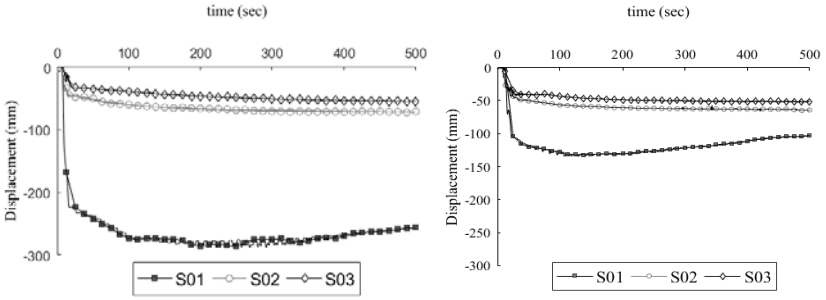

Figure 7 (a) Sinusoidal motion *Figure 7(b) Kocaeli Earthquake*

Figure 7. Liquefaction induced settlement in sand. Magnitudes at prototype scale.

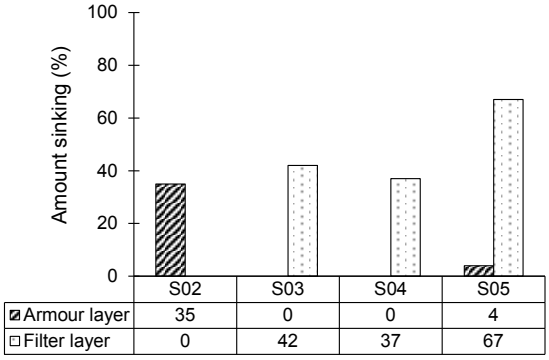

	S02	S03	S04	S05
Armour layer	35	0	0	4
Filter layer	0	42	37	67

Figure 8. Percentage of sinking of armour and filter layers for each model.

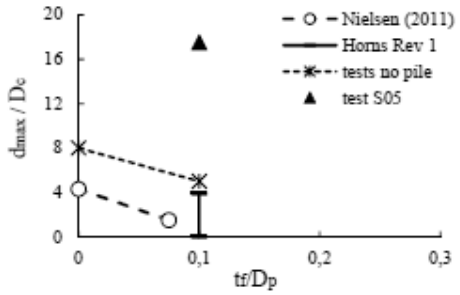

	t_f / D_p	D_a / D_p	D_f / D_p	t_a / D_c	t_f / D_f
Nielsen (2011)	0.075	0.09	0.06	1	1.4
Horns Rev 1	0.1	0.095	0.02	2.5	5
Current tests	0.1	0.1	0.02	2	5

Figure 9. Comparison between maximum sinking of scour protection for wave-induced settlement (Horns Rev 1 and Nielsen, 2011; Sumer & Nielsen, 2013), and earthquake-induced settlement.

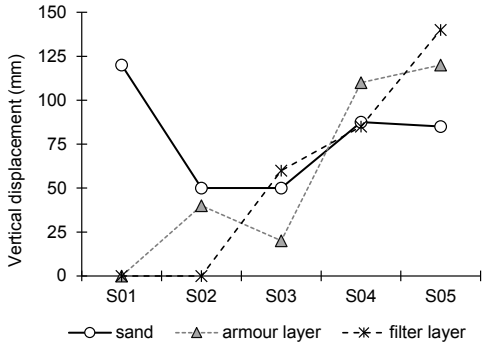

Figure 10. Settlement of layers in the middle of the model box.

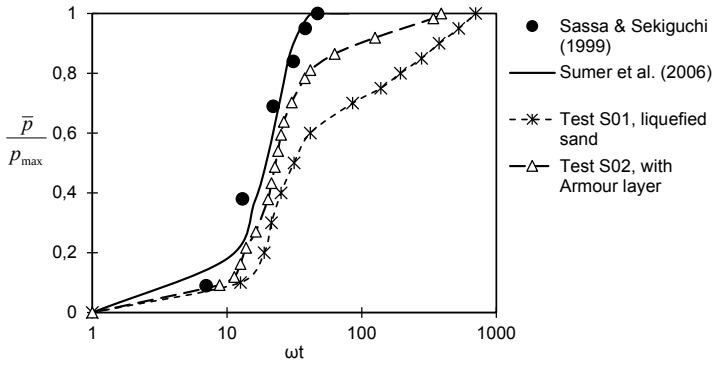

Figure 11. Comparison betwen Sassa and Sekiguchi's (1999) 50g centrifuge tests, Sumer et al's (2006) 1g standard wave-flume results, and this paper's 50g dynamic centrifuge tests.

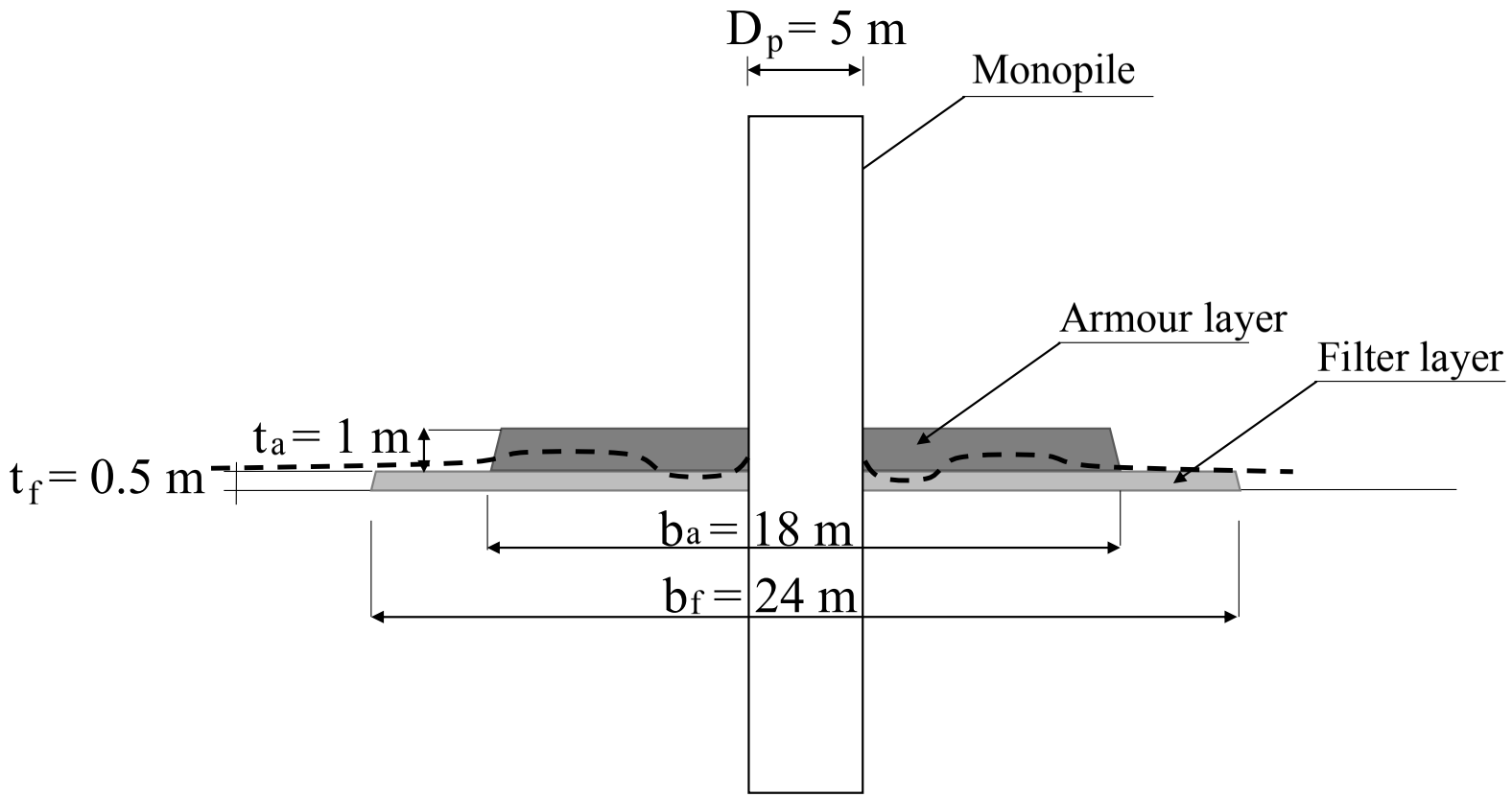
$D_p = 5$ m
Monopile
Armour layer
Filter layer
$t_a = 1$ m
$t_f = 0.5$ m
$b_a = 18$ m
$b_f = 24$ m

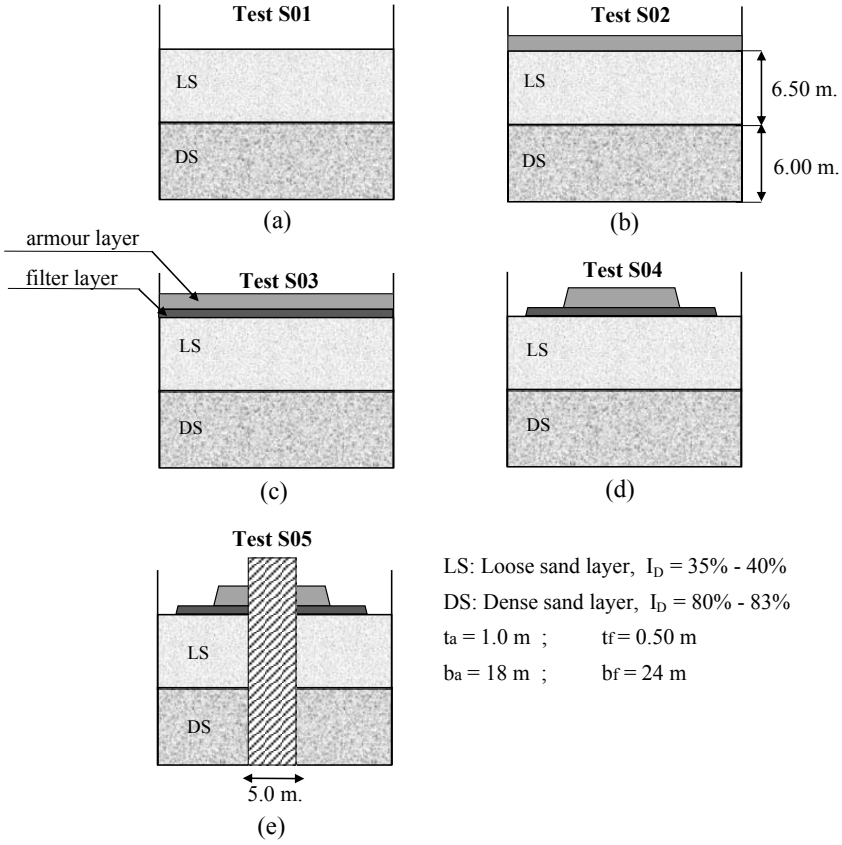

LS: Loose sand layer, I_D = 35% - 40%

DS: Dense sand layer, I_D = 80% - 83%

t_a = 1.0 m ; t_f = 0.50 m

b_a = 18 m ; b_f = 24 m

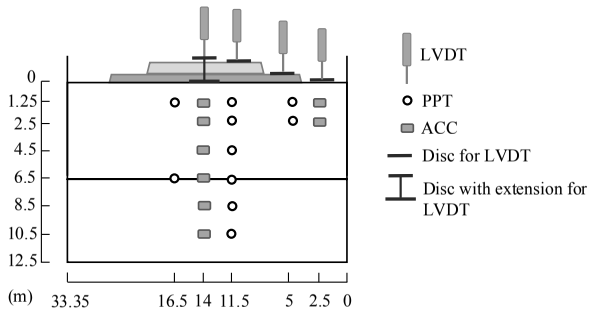
0
1.25
2.5
4.5
6.5
8.5
10.5
12.5
(m)
33.35
16.5
14
11.5
5
2.5
0
LVDT
PPT
ACC
Disc for LVDT
Disc with extension for LVDT

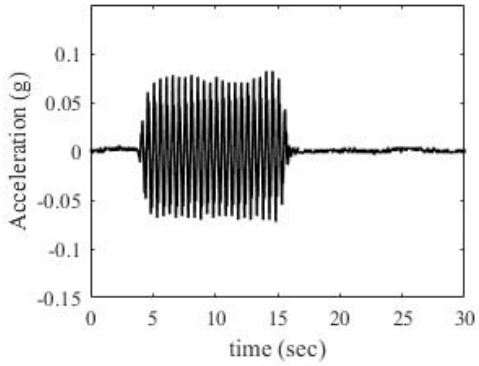
0.1
0.05
0
-0.05
-0.1
-0.15
Acceleration (g)
0
5
10
15
20
25
30
time (sec)

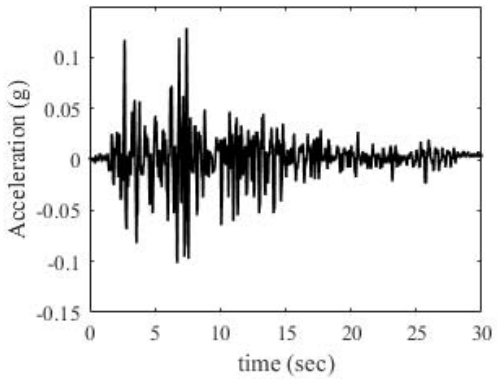
Acceleration (g)
0.1
0.05
0
-0.05
-0.1
-0.15
0
5
10
15
20
25
30
time (sec)

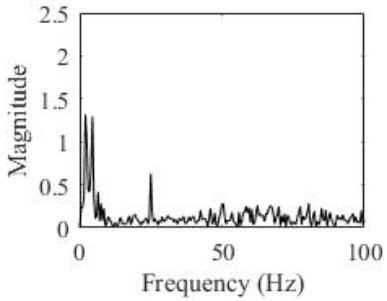
2.5
2
1.5
1
0.5
0
Magnitude
0
50
100
Frequency (Hz)

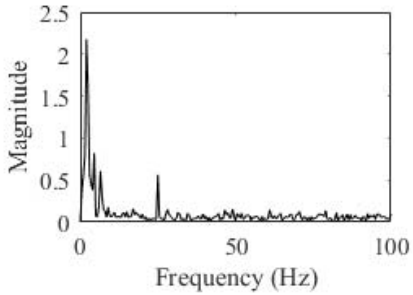
2.5
2
1.5
1
0.5
0
Magnitude
0
50
100
Frequency (Hz)

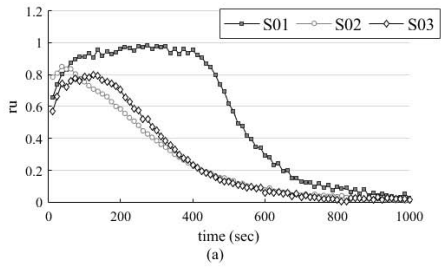

(a)

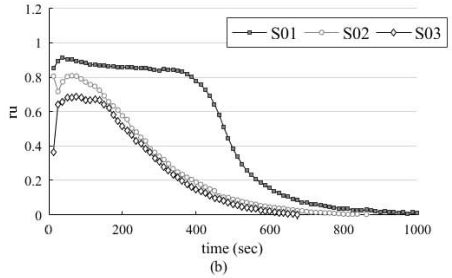

(b)

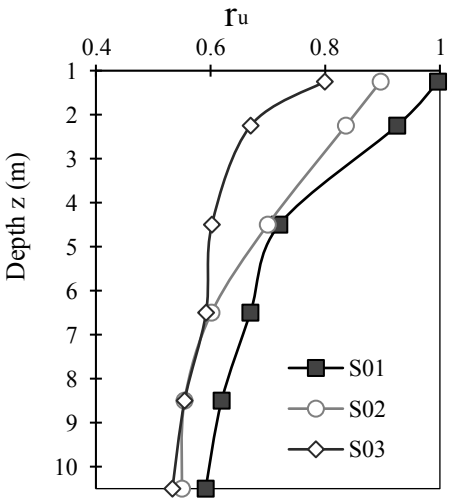
ru
0.4
0.6
0.8
1
Depth z (m)
1
2
3
4
5
6
7
8
9
10
S01
S02
S03

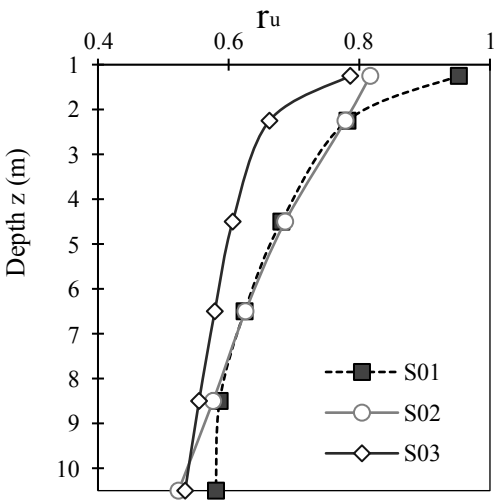
ru
0.4
0.6
0.8
1
Depth z (m)
1
2
3
4
5
6
7
8
9
10
S01
S02
S03

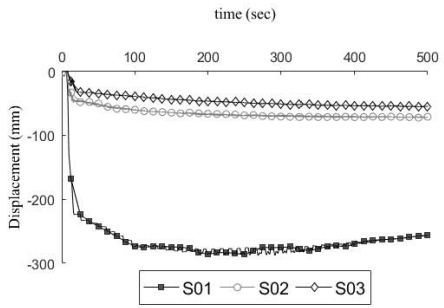
time (sec)
0
100
200
300
400
500
0
-100
-200
-300
Displacement (mm)
S01
S02
S03

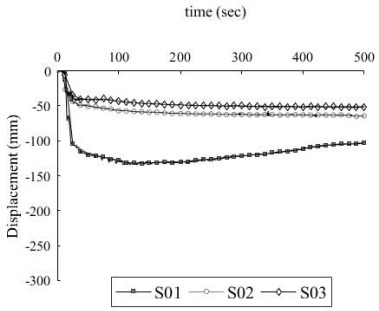
time (sec)
0
100
200
300
400
500
0
-50
-100
-150
-200
-250
-300
Displacement (mm)
S01
S02
S03

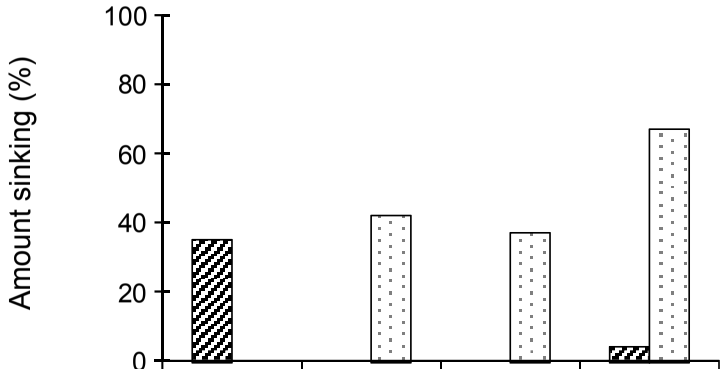

	S02	S03	S04	S05
Armour layer	35	0	0	4
Filter layer	0	42	37	67

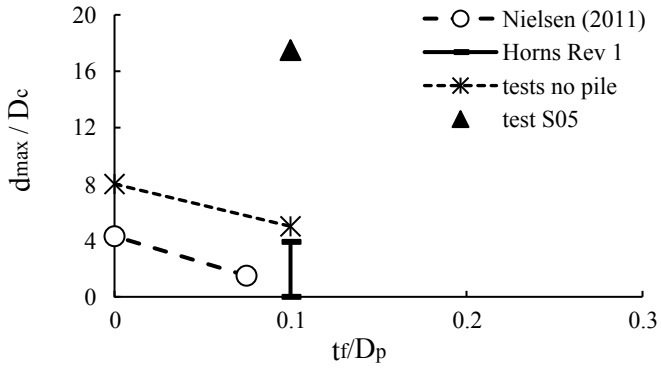

	t_f / D_p	D_a / D_p	D_f / D_p	t_a / D_c	t_f / D_f
Nielsen (2011)	0.075	0.09	0.06	1	1.4
Horns Rev 1	0.1	0.095	0.02	2.5	5
Current tests	0.1	0.1	0.02	2	5

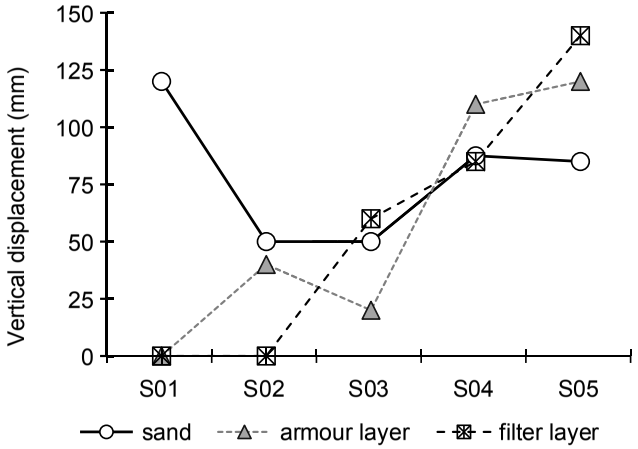
150
125
100
75
50
25
0
Vertical displacement (mm)
S01
S02
S03
S04
S05
sand
armour layer
filter layer

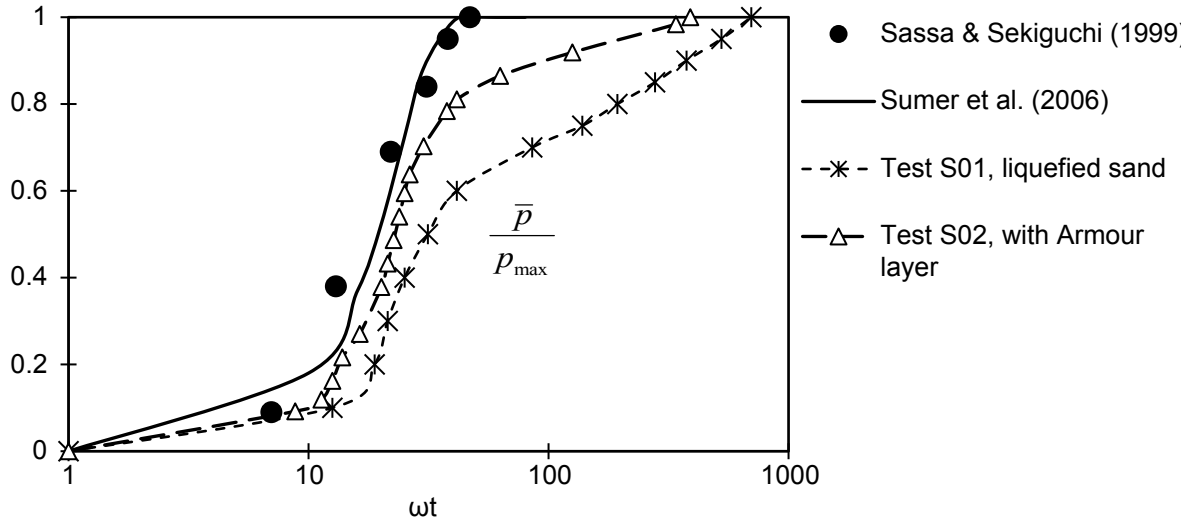
1
0.8
0.6
0.4
0.2
0
1
10
100
1000
ωt
$\frac{\overline{p}}{p_{\max}}$
Sassa & Sekiguchi (1999)
Sumer et al. (2006)
Test S01, liquefied sand
Test S02, with Armour layer

Property	Bertalot (2013)
D_{10} (mm)	0.07
D_{30} (mm)	0.10
D_{60} (mm)	0.146
C_u	1.96
G_s	2.63
$\gamma_{d,min}$ (kN/m^3)	14.34
$\gamma_{d,max}$ (kN/m^3)	17.60
e_{max}	0.795
e_{min}	0.463

Highlights

- A programme of centrifuge modelling was carried out to evaluate the stability of scour protection blankets over a liquefiable material.
- Scour protection blankets improve the response of a liquefiable sand under seismic loading.
- The stability of the scour protection blankets was highly improved by the use of a filter layer.
- Design guidelines should consider the presence of armour and filter layers in offshore foundations for areas prone to seismic action.